Using genetic algorithms to systematically improve the synthesis conditions of Al-PMOF

Nency P. Domingues,[†] Seyed Mohamad Moosavi,[†,‡] Leopold Talirz,[†,¶]

Christopher P. Ireland,[†] Fatmah Mish Ebrahim,[†] and Berend Smit[*,†]

†*Laboratory of Molecular Simulation (LSMO), Institut des Sciences et Ingénierie Chimiques, École Polytechnique Fédérale de Lausanne (EPFL), Rue de l'Industrie 17, CH-1951 Sion, Valais, Switzerland*

‡*Department of Mathematics and Computer Science, Freie Universität Berlin, Arnimallee 6, 14195 Berlin, Germany*

¶*Theory and Simulation of Materials (THEOS), School of Engineering (STI), École Polytechnique Fédérale de Lausanne (EPFL), CH-1015 Lausanne, Switzerland.*

E-mail: berend.smit@epfl.ch

Abstract

The synthesis of metal-organic frameworks (MOFs) is often complex and the desired structure is not always obtained. In this work, we report a methodology that uses a joint machine learning and experimental approach to obtain the optimal synthesis of a MOF. A synthetic conditions finder was used to derive the experimental protocols and a microwave based high-throughput robotic platform was used for the synthesis of Al-PMOF ($H_2TCPP[AlOH]_2(DMF_3(H_2O)_2)$). Al-PMOF was previously synthesized using a hydrothermal reaction, which gave a low throughput yield due to its relatively long reaction time (16 hours). In this work, we carried out a systematic search for the optimal reaction conditions using a microwave assisted reaction synthesis. For this

1

search we used a genetic algorithm and we show that already in the 2nd generation we obtained conditions that give excellent crystallinity and yield close to 80% in much shorter reaction time (50 minutes). In addition, by analysing the failed and partly successful experiments, we could identify the most important experimental variables that determine the crystallinity and yield.

Introduction

For the last two decades, metal-organic frameworks (MOFs) have been an extensive object of study[1–3] thanks to their high porosity[4–7] and their extensive spectrum of applications, including gas storage and separation, sensing, catalysis and drug delivery.[8–17] MOF synthesis consists of the self-assembly of the organic ligand and metal component into a periodic network.[18] Several methods for MOF synthesis have been developed including solvothermal, electrochemical, mechanochemical, microwave, and ultrasound.[8,16,19–21] In all these, one usually tries to find the optimal conditions at which crystals can form. Often this requires finding a sweet spot where the binding of the ligand and metal node is sufficiently strong that a stable crystal can form, but not too strong that the system quickly forms an amorphous structure which cannot be crystallized. In addition, different topologies may form[22] depending on the synthesis conditions.[23]

There are a considerable number of parameters that can influence the reaction and its outcome (i.e., solvents, pH, reagents concentration, reaction time, temperature, pressure, etc.),[24,25] and the optimization of these conditions for new or established MOFs is often laborious, expensive and time-consuming.[26,27] While conventionally, the optimization of these parameters rest on the chemical intuition of individuals, novel approaches are needed to tackle the extensive diversity in chemistry of MOFs.[28] Therefore, data-driven approaches have been developed to accelerate such optimization processes.[29–38] Moosavi et al.[29] combined a genetic algorithm (GA) with machine learning (ML) to optimise the synthesis of the MOFs. They illustrated their approach with the synthesis of HKUST-1[39] using a microwave-

based robotic platform, to find the synthesis conditions of HKUST-1 that yielded high quality crystals. This approach not only aims to find the optimal reaction conditions, but also aims to learn the most important experimental variables from analysing both successful, partly successful, and failed experiments.

In this work, we applied the Synthetic Conditions Finder (SyCoFinder),[40] which is the web-application based on the methodology developed by Moosavi et al.,[29] to find the optimal synthesis conditions for Al-PMOF ($H_2TCPP[AlOH]_2(DMF_3(H_2O)_2)$), first synthesized by Fateeva et al.[41] Unlike HKUST-1, our knowledge of alternative synthesis conditions of Al-PMOF is very limited. To the best of our knowledge, to date only one synthesis condition, a hydrothermal reaction, has been reported.[41] Unfortunately, this synthesis gives a relatively low yield (ca. 40%) with the reaction time of 16 hours.[41] Recently, there has been a renewed interest in this MOF as Boyd et al.[42] discovered that this material can efficiently capture CO_2 from wet flue gasses. However, the low yield and relatively long reaction time of the current reaction is at present a bottleneck to scale-up the synthesis. It is therefore important to investigate whether the yield and time of the reaction can be further optimized. In addition, it will give us some insights whether the approach developed by Moosavi et al. can be extended to other MOF systems.

Results

Experimental variables

The reported Al-PMOF synthesis is in pure water at a relatively high temperature (180 ºC).[41] We have carried out some attempts to synthesize Al-PMOF at a lower temperature or in pure dimethylformamide (DMF), which easily dissolves the ligand, but at these conditions we do not produce the MOF. If we repeat the synthesis in pure water, we obtained variable yields (40% to 90%) (Table S1). It is therefore interesting to systematically explore the synthesis conditions. For this purpose, we used our high-throughput microwave-based robotic platform

[63] (Figure S1).

[64] We start our first set of experiments (first generation) which aims at giving the most [65] diverse set in terms of experimental synthesis conditions. We explored the following set of [66] five variables:

[67] 1. Power of the microwave, by changing the power of the microwave we can influence the [68] time it takes the reaction solution to reach the required temperature;

[69] 2. Solvent composition, our solution has a fixed composition: 80% water and 20% of [70] an organic solvent, as it was found to be the most promising ratio from our previous [71] solvothermal attempts to increase the yield of the reaction (Table S2 and Figure S2) as [72] well as it presented a higher amount of an environmentally friendly solvent. [43] We tested [73] five different organic solvents that cover a range of different boiling points (from 75°C to [74] 190°C): ethanol (EtOH), 1-propanol, dimethylformamide (DMF), dimethylacetamide [75] (DMA) and dimethyl sulfoxide (DMSO);

[76] 3. Reaction time, which is the total time our vial was in the microwave (including both: [77] the time required to reach the temperature at which the reaction takes place ($<$ 1 [78] minute) and the reaction time itself);

[79] 4. Reaction temperature, the temperature at which the reaction is carried out;

[80] 5. Concentration of the reactants, the aluminium to porphyrin ratio was constant and set [81] as in the hydrothermal synthesis. [41] Concentrations 1 and 2 possess the same amount [82] of solvent but different amounts of precursors, while concentrations 2 and 3 possess the [83] same amount of precursors but different volumes (Table S3). This systematic approach [84] would allows us to assess the influence of each factor: concentration and pressure in [85] the reaction vial.

[86] The ranges of these variables were based on our experience with the solvothermal synthesis [87] of Al-PMOF and are detailed in Table 1. In contrast to our previous work where we used

4

one-hot encoding for solvent type, here, we describe solvents with a continuous variable to better interpolate between different solvent types. The boiling point of the solvent is a good descriptor as it is important for solvothermal synthesis.[20]

Table 1: Table showing the synthetic variables, their ranges and importance based on our chemical intuition from the solvothermal synthesis. The concentration was given discrete variables: 1, 2, and 3 corresponding to high, medium, and low concentration, respectively (see Table S3 for experimental details).

Variable	Range	Importance
Power [W]	200 to 300	1.48
Temperature [°C]	175 to 200	4.47
Time [min]	20 to 60	4.47
Concentration [-]	1 to 3	4.90
Boiling Point [°C]	80 to 190	6.46

Design of the experimental protocols with the SyCoFinder

Based on the range of the variables given in Table 1, we used the SyCoFinder[40] to generate a set of 25 most diverse experiments (Table S4). In the first generation, variables are weighted based on the chemical intuition from the solvothermal synthesis, as listed in Table 1. The type of solvent (i.e., boiling point) was deemed to be the most important variable. Reaction temperature, time and concentration were thought to play a slightly less important role, and power the least important of all the variables studied. These 25 reactions were carried out utilising the microwave and robotic platform (Figure S1). After synthesis, each sample was collected individually by centrifugation, washed with the organic solvent used for the reaction itself and then dried overnight in a ventilated oven at 60°C.

Crystalline structure and yield

The resulting reactions produce vastly different results; a number of experiments yielded little or no powder, and many were amorphous. The powder X-ray diffraction (PXRD) pattern was collected, showing very distinct crystallinity for the best and worst samples (Figure 1).

Seven reactions from the first generation yielded a PXRD pattern characteristic of Al-PMOF. The crystallinity was ranked on a scale of 1 to 10, where 1 was used for samples that did not yield a powder, 2-5 was for samples that were amorphous or had poor crystallinity, while higher numbers were given to powders which presented better crystallinity. Distinctions between 9 and 10 were made for those which presented additional peaks or fully matched the Al-PMOF predicted pattern without any additional phase or impurities, respectively.
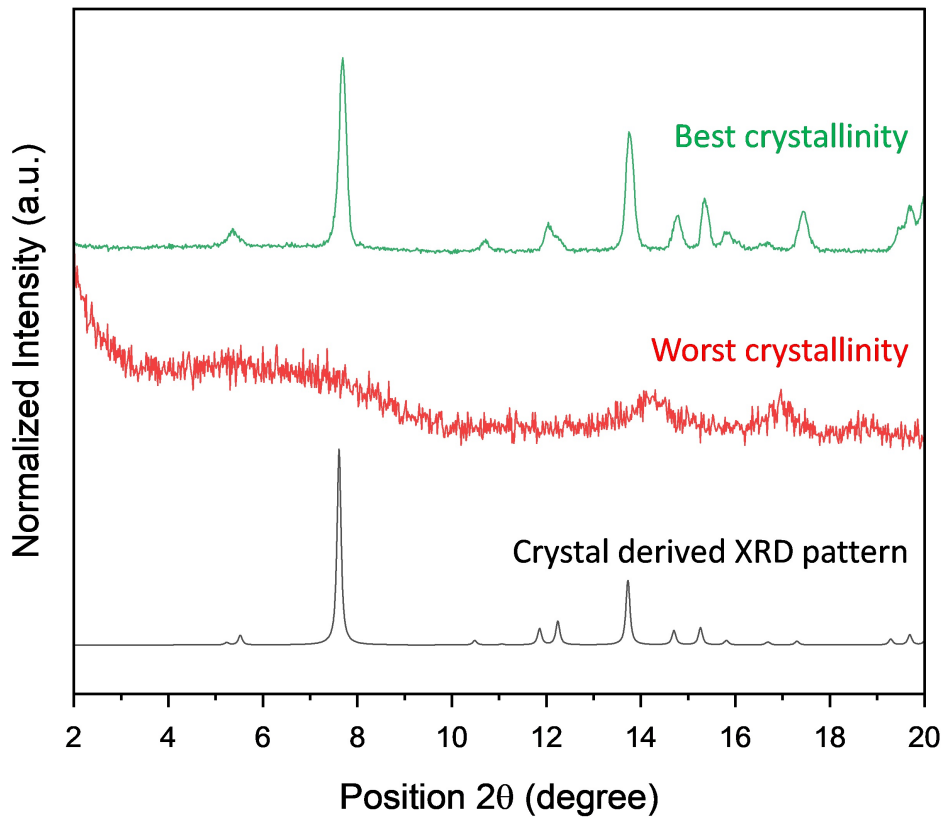
Figure 1: PXRD of the best and worst samples produced from the first generation of experiments, with the crystal derived predicted pattern of Al-PMOF from the CIF file.

The ranking from the first generation (Figure 4) was used to further optimise the synthesis by generating a second generation of experiments with the genetic algorithm of SyCoFinder (Table S5). Again, after synthesis, the PXRD patterns were gathered and the experimental results were ranked. Interestingly, in this second generation, all of the material synthesised

proved to be crystalline and matched the PXRD pattern of Al-PMOF (Figure 2).

Our initial aim was to screen for both crystallinity and yield. As already after the first generation we obtained a near perfect score on crystallinity, we could already rank our reaction conditions based on yield. We determined the yield by weighing the powder obtained divided by the amount of porphyrin ligand used in the synthesis, which gives a good indication of what the actual yield would be. Interestingly, a number of conditions gave excellent results, with a high yield and good crystallinity (Figures 2 and 4). As the crystallinity and yield where sufficiently high and the surface area similar to what was obtained previously, there was no need for a 3$^{\text{rd}}$ generation of experiments.
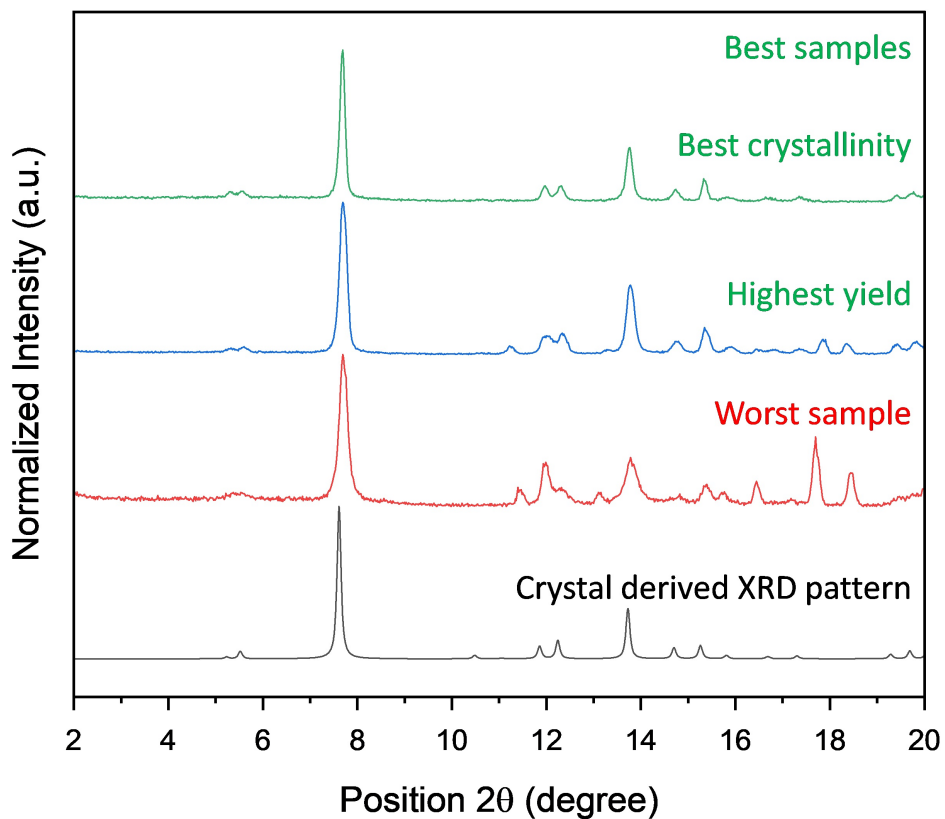

Figure 2: PXRD of the best (highest crystallinity and yield) and worst samples produced from the second generation of experiments, with the crystal derived predicted pattern of Al-PMOF from the CIF file.

For carbon capture applications it is important that the pore structure is the same as the solvothermal synthesis. As a high-throughput technique, we determined the surface area from a nitrogen (N_2) isotherm at 77 K for the highest ranked materials (samples 4 and 15 from generation 2). From these isotherms, we obtained surface areas (1236 m^2 g^{-1}) comparable to that previously reported with a hydrothermal synthesis (i.e., 1400 m^2 g^{-1}),[41] which indicates it is likely that the robot synthesized material has retained the pore structure of the MOF, and so, it should be suitable for CO_2 capture applications.

Reproducibility and large MOF synthesis

The reproducibility of the highest ranking synthesis conditions were also tested, with the robotic platform set up to run 16 reactions over a 24 hour period. The powder was collected by centrifuge, and then washed with solvent and dried overnight. The combined PXRD pattern matched Al-PMOF perfectly, and the surface area and pore volume of the large sample determined from a N_2 isotherm at 77K were also comparable. Continuously synthesising using the platform this way can generate gram amounts of powder that can be used for further applications such as CO_2 capture at a large scale.

Discussion

Analysis of the experimental variables

In Figure 4, we have summarized the results of this study. And in Figure 3 we show, through analysis of the failed and partially successful experiments, the relative importance of the experimental variables in obtaining (a) high crystallinity, and (b) high yield, as obtained from the machine learning module in the SyCoFinder. From our analysis, we see that the changes of concentration of reactants followed by changes in the solvent have the most impact on crystallinity. While for the yield, by far the most important criteria is the solvent type.
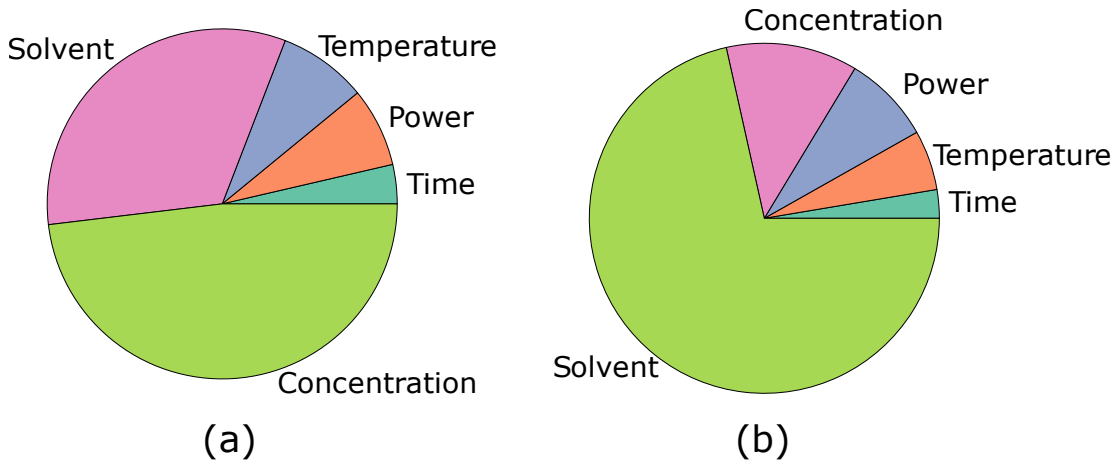
8

Figure 3: Pie charts showing the relative importance of each synthesis variable on (a) crystallinity, (b) yield.

Influence of the solvent

The standard hydrothermal procedure for the synthesis of this MOF shows that, although synthesized in pure water, a higher temperature (i.e., 180°C) is required to dissolve the porphyrin and allow it to react with the aluminium precursor. Using a mixture of water and another organic solvent could help the porphyrin to dissolve, whilst retaining the high heat capacity of water which seems to be required to form the MOF. Solvothermal reactions with different H_2O:DMF ratios (i.e., 20:80%, 50:50%, and 80:20%) were carried out (see supplementary information for experimental details) and the optimal results were obtained with a 80:20% H_2O:DMF ratio (Table S2 and Figure S2). DMF is a common solvent for MOF synthesis,[44] due to its high dielectric constant and relatively high boiling point. It is interesting to look in some detail at the second generation of experiments that were proposed by SyCoFinder's algorithm. In the first generation, DMF was included as additional organic solvent, yet the second generation of reactions did not include any experiments with DMF. This is due to the fact that the crystallinity of samples with DMF are poor, and the other solvents yielded higher crystallinity. The analysis of the data shows that the solvent type, which we characterize by the boiling point, is one of the key variables that determine the

9

crystallinity. The data also show that, although the type of solvent is important, the quality of the crystals does not linearly correlate with the boiling point. Yield might be better described by this factor: higher boiling point solvents (i.e., DMSO) show a much lower yield, while lower boiling point solvents (i.e., EtOH) show a higer one (Figure 4).

Influence of the concentration

The concentration of the precursors was also studied: Al-PMOF was obtained with the same metal to ligand ratio except for different amounts of solvent, which also leads to a change of the pressure inside the reaction vessel. As a control, concentrations 1 and 2, possess the same volume but different metal and ligand concentrations (Table S3). The analysis of the relative importance of experimental variables shows that concentration plays a major role on crystallinity. The lowest concentration (i.e., concentration 3, which also presents the largest amount of solvent, and thus highest pressure) is not suggested in generation 2, as it leads to relatively poor crystallinities in generation 1. It seems that the combination of low concentrations and high pressures in the reaction vessel are not beneficial for the MOF formation. On the other hand, if we compare concentrations 1 and 2, which possess the same volume, the highest concentration (i.e., concentration 1) tends to give better crystallinities overall, which may be positively correlated to the kinetics of the reaction[45] (Figure 4).
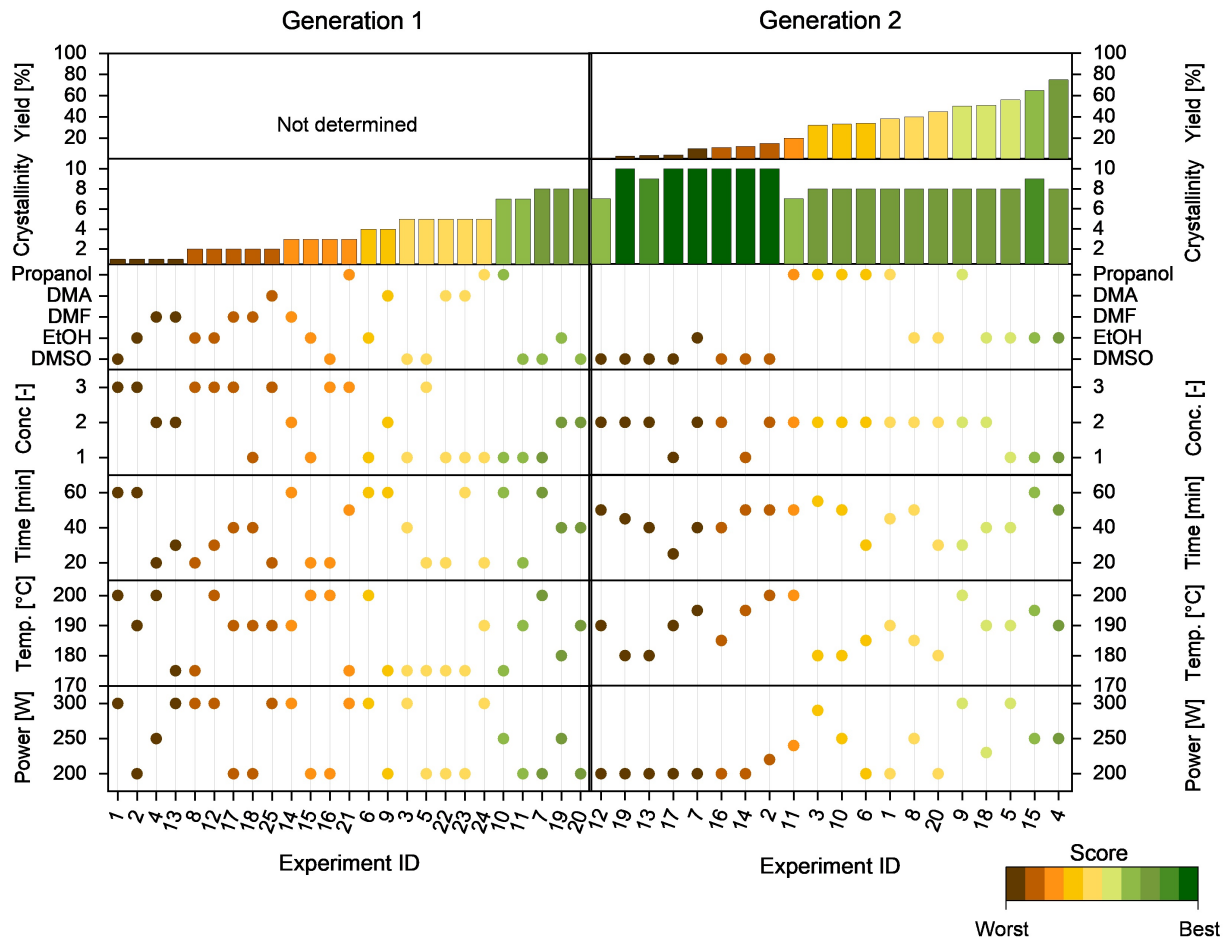
Figure 4: Parameters and results of optimization with microwave power, reaction temperature, time, concentration and solvents selected for each Al-PMOF synthesis. Color code is given for worst (brown) and best (dark green) samples. Generation 1 was ranked in terms of the crystallinity of each sample, while the success of generation 2 was determined by the yield as all samples proved to be highly crystalline. This proves the success of the GA in providing good crystallinity of all samples in just one generation.

Influence of other variables

The other variables studied (i.e., reaction time, temperature and power of the microwave) were deemed to be less important for both analyses: crystallinity and yield of Al-PMOF synthesis (Figure 3). These were adapted to our needs (i.e., low reaction time) and had been tuned according to our knowledge of the hydrothermal synthesis (i.e., reaction temperature), while the power was limited by our microwave reactor.

11

Conclusions

In summary, we have developed an alternative Al-PMOF synthesis method, using a microwave reactor with comparable crystallinity and surface area to the traditional Al-PMOF hydrothermal synthesis, but with a higher yield and a much shorter reaction time.

The other interesting part of this work, is the methodology which we used to find the optimal synthesis conditions: an experimental design which learns from the failed and partly successful experiments. Although we used a robot in this work, the total number of experiments that were used to find these conditions, only two generations and total of 45 experiments, illustrate that the underlying methodology does not require very large data sets to be of practical use.

We hope that our results encourage authors to publish their failed and partially successful experiments. The fact that we only publish the successful recipes creates a bias in the literature, that makes predictions of the reaction conditions using machine learning more difficult.[46] Of course, in our case, as we are using a robot, publishing the failed and partially successful conditions in addition to the successful recipe does not create an additional burden. Jablonka et al.[46] outline some ideas on how the burden of reporting of all experimental results can be facilitated.

Methods

Characterization

Powder X-ray diffraction (PXRD) patterns of all samples were collected on a Bruker D8 Advance diffractometer at ambient temperature using monochromated Cu Kα radiation (λ = 1.5418 Å), with a 2θ step of 0.02° with different 2θ ranges. Simulated PXRD patterns were generated from the corresponding crystal structures using Mercury 3.0.

The N$_2$ adsorption isotherm measurements were performed at 77 K using a BELSORP

Mini (BEL Japan, Inc.). Prior to measurements, samples were activated at 180 °C for 12 hours under dynamic vacuum. The N_2 adsorption isotherm in the $p/p0$ range 0.06 − 0.25 was fitted to the Brunauer–Emmett–Teller (BET) equation to estimate the surface area of the samples.

Chemical synthesis

Detailed protocols for each Al-PMOF synthesis performed in this study can be found in the supplementary information.

Acknowledgement

Author contributions

N.P.D. and C.P.I. conceived this study and planned the experiments. N.P.D. performed the experiments. N.P.D., C.P.I., S.M.M., L.T. and F.M.E. were involved in the the data analysis

and interpretation. C.P.I., B.S., N.P.D., and S.M.M. wrote the manuscript. All authors read and commented on the manuscript.

Competing interests

The authors declare no competing interests.

Supporting Information Available

The characterization data (including powder X-ray (PXRD) patterns and N_2 isotherms at 77K) is saved in the electronic lab notebook (ELN).[46–48] The spectra are usually stored in JCAMP-DX format and the sample information with metadata in JavaScript Object Notation (JSON). The characterisation data is available on Zenodo (DOI: 10.5281/zenodo.6616402) and can be visualised through the following view developed with the visualizer library : `https://www.cheminfo.org/flavor/zenodo/index.html?id=6620502`.[49]

References

(1) Dai, S.; Tissot, A.; Serre, C. Metal-Organic Frameworks: from ambient green synthesis to applications. *Bulletin of the Chemical Society of Japan* **2021**, *94*, 2623–2636.

(2) Meng, J.; Liu, X.; Niu, C.; Pang, Q.; Li, J.; Liu, F.; Liu, Z.; Mai, L. Advances in metal–organic framework coatings: versatile synthesis and broad applications. *Chemical Society Reviews* **2020**, *49*, 3142–3186.

(3) Ockwig, N. W.; Delgado-Friedrichs, O.; O'Keeffe, M.; Yaghi, O. M. Reticular chemistry: occurrence and taxonomy of nets and grammar for the design of frameworks. *Accounts of chemical research* **2005**, *38*, 176–182.

(4) Zhang, X.; Chen, Z.; Liu, X.; Hanna, S. L.; Wang, X.; Taheri-Ledari, R.; Maleki, A.; Li, P.; Farha, O. K. A historical overview of the activation and porosity of metal–organic frameworks. *Chemical Society Reviews* **2020**, *49*, 7406–7427.

(5) Liu, X.; Zhang, L.; Wang, J. Design strategies for MOF-derived porous functional materials: Preserving surfaces and nurturing pores. *Journal of Materiomics* **2021**, *7*, 440–459.

(6) Li, H.; Eddaoudi, M.; O'Keeffe, M.; Yaghi, O. M. Design and synthesis of an exceptionally stable and highly porous metal-organic framework. *nature* **1999**, *402*, 276–279.

(7) Furukawa, H.; Ko, N.; Go, Y. B.; Aratani, N.; Choi, S. B.; Choi, E.; Yazaydin, A. Ö.; Snurr, R. Q.; O'Keeffe, M.; Kim, J., et al. Ultrahigh porosity in metal-organic frameworks. *Science* **2010**, *329*, 424–428.

(8) Horcajada, P.; Gref, R.; Baati, T.; Allan, P. K.; Maurin, G.; Couvreur, P.; Ferey, G.; Morris, R. E.; Serre, C. Metal–organic frameworks in biomedicine. *Chemical reviews* **2012**, *112*, 1232–1268.

(9) Cunha, D.; Ben Yahia, M.; Hall, S.; Miller, S. R.; Chevreau, H.; Elkaïm, E.; Maurin, G.; Horcajada, P.; Serre, C. Rationale of drug encapsulation and release from biocompatible porous metal–organic frameworks. *Chemistry of Materials* **2013**, *25*, 2767–2776.

(10) Li, B.; Wen, H.-M.; Cui, Y.; Zhou, W.; Qian, G.; Chen, B. Emerging multifunctional metal–organic framework materials. *Advanced Materials* **2016**, *28*, 8819–8860.

(11) Freund, R.; Zaremba, O.; Arnauts, G.; Ameloot, R.; Skorupskii, G.; Dincǎ, M.; Bavykina, A.; Gascon, J.; Ejsmont, A.; Goscianska, J., et al. The current status of MOF and COF applications. *Angewandte Chemie International Edition* **2021**, *60*, 23975–24001.

(12) Jiao, L.; Wang, Y.; Jiang, H.-L.; Xu, Q. Metal–organic frameworks as platforms for catalytic applications. *Advanced Materials* **2018**, *30*, 1703663.

(13) Sumida, K.; Rogow, D. L.; Mason, J. A.; McDonald, T. M.; Bloch, E. D.; Herm, Z. R.; Bae, T.-H.; Long, J. R. Carbon dioxide capture in metal–organic frameworks. *Chemical reviews* **2012**, *112*, 724–781.

(14) Jiao, L.; Seow, J. Y. R.; Skinner, W. S.; Wang, Z. U.; Jiang, H.-L. Metal–organic frameworks: Structures and functional applications. *Materials Today* **2019**, *27*, 43–68.

(15) Xiao, J.-D.; Jiang, H.-L. Metal–organic frameworks for photocatalysis and photothermal catalysis. *Accounts of Chemical Research* **2018**, *52*, 356–366.

(16) Soni, S.; Bajpai, P. K.; Arora, C. A review on metal-organic framework: Synthesis, properties and ap-plication. *Characterization and Application of Nanomaterials* **2020**, *3*, 87–106.

(17) Vitillo, J. G.; Smit, B.; Gagliardi, L. Introduction: Carbon Capture and Separation. *Chem. Rev.* **2017**, *117*, 9521–9523.

(18) Yaghi, O. M.; O'Keeffe, M.; Ockwig, N. W.; Chae, H. K.; Eddaoudi, M.; Kim, J. Reticular synthesis and the design of new materials. *Nature* **2003**, *423*, 705–714.

(19) MacGillivray, L. *Design and Application*; Wiley: Hoboken, N.J., 2010.

(20) Stock, N.; Biswas, S. Synthesis of metal-organic frameworks (MOFs): routes to various MOF topologies, morphologies, and composites. *Chemical reviews* **2012**, *112*, 933–969.

(21) Lee, Y.-R.; Kim, J.; Ahn, W.-S. Synthesis of metal-organic frameworks: A mini review. *Korean Journal of Chemical Engineering* **2013**, *30*, 1667–1680.

(22) Zhou, H.-C.; Long, J. R.; Yaghi, O. M. Introduction to metal–organic frameworks. 2012.

(23) Anderson, S. L.; Tiana, D.; Ireland, C. P.; Capano, G.; Fumanal, M.; Gładysiak, A.; Kampouri, S.; Rahmanudin, A.; Guijarro, N.; Sivula, K., et al. Taking lanthanides out of isolation: tuning the optical properties of metal–organic frameworks. *Chemical science* **2020**, *11*, 4164–4170.

16

(24) Kareem, H. M.; Abd Alrubaye, R. T. Synthesis and Characterization of Metal Organic Frameworks for Gas Storage. IOP Conference Series: Materials Science and Engineering. 2019; p 062013.

(25) Wu, R.; Fan, T.; Chen, J.; Li, Y. Synthetic factors affecting the scalable production of zeolitic imidazolate frameworks. *ACS Sustainable Chemistry & Engineering* **2019**, *7*, 3632–3646.

(26) Xu, J.; Liu, J.; Li, Z.; Wang, X.; Xu, Y.; Chen, S.; Wang, Z. Optimized synthesis of Zr (IV) metal organic frameworks (MOFs-808) for efficient hydrogen storage. *New Journal of Chemistry* **2019**, *43*, 4092–4099.

(27) Mulyati, T. A.; Ediati, R.; Nadjib, M. Optimization of Reaction Conditions for Synthesis of MOF-5 using Solvothermal Method. *IPTEK Journal of Proceedings Series* **2015**, *1*.

(28) Moosavi, S. M.; Nandy, A.; Jablonka, K. M.; Ongari, D.; Janet, J. P.; Boyd, P. G.; Lee, Y.; Smit, B.; Kulik, H. Understanding the diversity of the metal-organic framework ecosystem. *Nature Communications* **2020**, *11*, 4068.

(29) Moosavi, S. M.; Chidambaram, A.; Talirz, L.; Haranczyk, M.; Stylianou, K. C.; Smit, B. Capturing chemical intuition in synthesis of metal-organic frameworks. *Nature communications* **2019**, *10*, 1–7.

(30) Aldeghi, M.; Hase, F.; Hickman, R. J.; Tamblyn, I.; Aspuru-Guzik, A. Golem: an algorithm for robust experiment and process optimization. *Chem Sci* **2021**, *12*, 14792–14807.

(31) Christensen, M.; Yunker, L. P. E.; Adedeji, F.; Hase, F.; Roch, L. M.; Gensch, T.; Gomes, G. D.; Zepel, T.; Sigman, M. S.; Aspuru-Guzik, A.; Hein, J. E. Data-science driven autonomous process optimization. *Commun Chem* **2021**, *4*.

(32) Hase, F.; Aldeghi, M.; Hickman, R. J.; Roch, L. M.; Aspuru-Guzik, A. Gryffin: An algo-rithm for Bayesian optimization of categorical variables informed by expert knowledge. *Appl Phys Rev* **2021**, *8*.

(33) Xie, Y.; Zhang, C.; Deng, H.; Zheng, B.; Su, J.-W.; Shutt, K.; Lin, J. Accelerate Synthe-sis of Metal–Organic Frameworks by a Robotic Platform and Bayesian Optimization. *ACS Applied Materials & Interfaces* **2021**, *13*, 53485–53491.

(34) Duros, V.; Grizou, J.; Xuan, W.; Hosni, Z.; Long, D.-L.; Miras, H. N.; Cronin, L. Human versus robots in the discovery and crystallization of gigantic polyoxometalates. *Angewandte Chemie* **2017**, *129*, 10955–10960.

(35) Raccuglia, P.; Elbert, K. C.; Adler, P. D.; Falk, C.; Wenny, M. B.; Mollo, A.; Zeller, M.; Friedler, S. A.; Schrier, J.; Norquist, A. J. Machine-learning-assisted materials discovery using failed experiments. *Nature* **2016**, *533*, 73–76.

(36) Zhou, Z.; Li, X.; Zare, R. N. Optimizing chemical reactions with deep reinforcement learning. *ACS central science* **2017**, *3*, 1337–1344.

(37) Jablonka, K. M.; Ongari, D.; Moosavi, S. M.; Smit, B. Big-data science in porous ma-terials: materials genomics and machine learning. *Chemical reviews* **2020**, *120*, 8066–8129.

(38) Moosavi, S. M.; Jablonka, K. M.; Smit, B. The role of machine learning in the under-standing and design of materials. *Journal of the American Chemical Society* **2020**, *142*, 20273–20287.

(39) Chui, S. S.-Y.; Lo, S. M.-F.; Charmant, J. P.; Orpen, A. G.; Williams, I. D. A chemically functionalizable nanoporous material [Cu3 (TMA) 2 (H2O) 3] n. *Science* **1999**, *283*, 1148–1150.

(40) S.M. Moosavi, L. T.; Smit, B. Synthesis condition finder. 2019; `https://www.materialscloud.org/work/tools/sycofinder`.

(41) Fateeva, A.; Chater, P. A.; Ireland, C. P.; Tahir, A. A.; Khimyak, Y. Z.; Wiper, P. V.; Darwent, J. R.; Rosseinsky, M. J. A water-stable porphyrin-based metal-organic framework active for visible-light photocatalysis. *Angewandte Chemie International Edition* **2012**, *51*, 7440–7444.

(42) Boyd, P. G. et al. Data-driven design of metal-organic frameworks for wet flue gas CO2 capture. *Nature* **2019**, *576*, 253–+.

(43) Kumar, S.; Jain, S.; Nehra, M.; Dilbaghi, N.; Marrazza, G.; Kim, K.-H. Green synthesis of metal–organic frameworks: A state-of-the-art review of potential environmental and medical applications. *Coordination Chemistry Reviews* **2020**, *420*, 213407.

(44) Park, H.; Kang, Y.; Choe, W.; Kim, J. Mining Insights on Metal–Organic Framework Synthesis from Scientific Literature Texts. *Journal of Chemical Information and Modeling* **2022**, *62*, 1190–1198.

(45) McKinstry, C.; Cussen, E. J.; Fletcher, A. J.; Patwardhan, S. V.; Sefcik, J. Effect of synthesis conditions on formation pathways of metal organic framework (MOF-5) crystals. *Crystal growth & design* **2013**, *13*, 5481–5486.

(46) Jablonka, K. M.; Patiny, L.; Smit, B. Making the collective knowledge of chemistry open and machine actionable. *Nat Chem* **2022**, *14*, 365–376.

(47) Patiny, L.; Zasso, M.; Kostro, D.; Bernal, A.; Castillo, A. M.; Bolaños, A.; Asencio, M. A.; Pellet, N.; Todd, M.; Schloerer, N., et al. The C6H6 NMR repository: an integral solution to control the flow of your data from the magnet to the public. *Magnetic Resonance in Chemistry* **2018**, *56*, 520–528.

(48) Jablonka, K. M.; Moosavi, S. M.; Asgari, M.; Ireland, C.; Patiny, L.; Smit, B. A data-driven perspective on the colours of metal–organic frameworks. *Chemical science* **2021**, *12*, 3587–3598.

(49) Pellet, N. jsGraph and jsNMR—advanced scientific charting. *Challenges* **2014**, *5*, 294–295.